

# Precision measurement of the metastable $^3P_2$ lifetime of neon

Martin Zinner, Peter Spoden, Tobias Kraemer, Gerhard Birkel\*, and Wolfgang Ertmer  
*Institut für Quantenoptik, Universität Hannover, Welfengarten 1, D-30167 Hannover*

(Dated: June 18, 2021)

The lifetime of the metastable  $^3P_2$  state of neon has been determined to 14.70(13) s (decay rate  $0.06801(62) \text{ s}^{-1}$ ) by measuring the decay in fluorescence of an ensemble of  $^{20}\text{Ne}$  atoms trapped in a magneto-optical trap (MOT). Due to low background gas pressure ( $p < 5 \times 10^{-11} \text{ mbar}$ ) and low relative excitation to the  $^3D_3$  state (0.5 % excitation probability) operation only small corrections have to be included in the lifetime extrapolation. Together with a careful analysis of residual loss mechanisms in the MOT a lifetime determination to high precision is achieved.

PACS numbers: 32.70.Cs, 32.70.Fw, 32.80.Pj

In contrast to its importance for various active fields of research covering such a wide range as atomic physics, quantum optics, and nuclear physics, there still has been no measurement of the natural lifetime of the metastable  $^3P_2$  state [1] of neon with sufficient precision. A selection of research activities profiting from an improved measurement include the quest for Bose-Einstein condensation (BEC) of metastable neon, advanced atomic structure calculations, the investigation of ultracold collisions, and even precision tests of the electroweak theory being currently pursued by investigating the nuclear decay of an optically trapped sample of  $^{19}\text{Ne}$  in the  $^3P_2$  state [2].

Ongoing research directed towards BEC of metastable neon atoms in the  $^3P_2$  state [3, 4] clearly will benefit from an accurate knowledge of the state's lifetime. This includes the optimization of the production process as well as the study of collision processes such as Penning-ionization [5] and elastic s-wave scattering. Exciting new physics complementing the work on metastable helium [6, 7] can be expected for a  $^3P_2$  neon condensate. We would like to point out the study of higher-order correlations [8] and the intriguing possibility of a modification of the  $^3P_2$  decay rate due to the high phase-space density or the phase coherence in a BEC [9].

Significant advance in atomic structure calculations has already been and will be further triggered [10] by the work presented here. To date only a preliminary experimental value of 22 s for the  $^3P_2$  lifetime of neon exists [11] with no detailed investigations having been performed [12]. A precise determination of the lifetime will put a more stringent test on theory. For most rare-gas atoms, the  $^3P_2$  lifetime depends sensitively on electron correlations and relativistic corrections. The latter have only a minor effect for the case of neon, making neon specifically interesting for a critical test of electron correlations. In addition, our measurement will close the chain of  $^3P_2$  lifetime measurements for rare-gas atoms beyond helium performed in recent years for Ar ( $38_{-5}^{+8} \text{ s}$  [13]), Kr ( $39_{-4}^{+5} \text{ s}$  [13] and  $28.3_{-1.8}^{+1.8} \text{ s}$  [14]), and Xe ( $42.9_{-0.9}^{+0.9} \text{ s}$  and  $42.4_{-1.3}^{+1.3} \text{ s}$  [15]), respectively. This will deliver the

input for a detailed systematic investigation of the Z-dependence of metastable lifetimes.

An accurate experimental determination of the  $^3P_2$  lifetimes of rare-gas atoms other than helium has only been achievable by the ability to prepare cold atom samples in a MOT [11, 13, 14, 15]. For a precision lifetime measurement, the coupling of the  $^3P_2$  to the  $^3D_3$  state by the MOT light has to be considered since it will modify the observed decay rate. To date, two different methods making use of a variable MOT-on/off duty cycle have been employed, either by directly measuring the rate of UV photons produced by the decay during a MOT-off period [14, 15] or by extrapolating the observed decay rate for varying MOT-on/off duty ratios to vanishing MOT-on periods [13].

In our approach, we record the decay of fluorescence in a MOT (Fig. 1) for different steady-state values of the population  $\pi_3$  of the  $^3D_3$  state ( $0.005 < \pi_3 < 0.47$ ). This allows the extrapolation of the observed decay rate to  $\pi_3 = 0$  thus giving the  $^3P_2$  lifetime. Extreme care has been taken to achieve optimized experimental conditions such as low background gas pressure ( $p < 5 \times 10^{-11} \text{ mbar}$ ) and MOT operation for such low values as  $\pi_3 = 0.005$ . This minimizes the amount of required corrections dra-

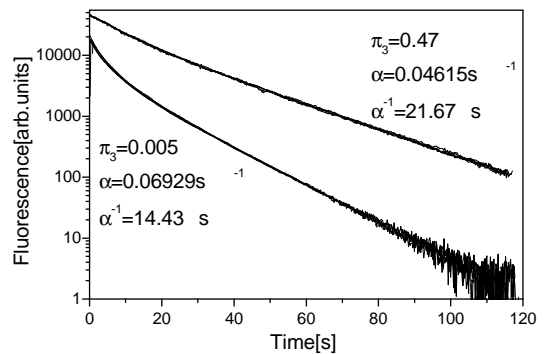


FIG. 1: Decay of the fluorescence for a  $^{20}\text{Ne}$  ensemble in a MOT for the given excitations to the  $^3D_3$  state of  $\pi_3 = 0.005$  ( $\Delta/\Gamma = -5.3$ ,  $I/I_0 = 1.75$ ,  $p = 3.4 \times 10^{-11} \text{ mbar}$ ) and  $\pi_3 = 0.47$  ( $\Delta/\Gamma = -0.16$ ,  $I/I_0 = 24$ ,  $p = 4.7 \times 10^{-11} \text{ mbar}$ ). Both sets of data consist of five curves each, demonstrating the high reproducibility of our decay measurements.

\* Author to whom correspondence should be addressed.

matically and the accuracy to which the  $^3\text{P}_2$  lifetime of Ne can be determined is improved considerably.

With no observable changes in shape and temperature of the atom sample, the temporal evolution of the observed fluorescence is proportional to the temporal evolution of the number of trapped atoms  $N(t)$ . The decay can be described by the differential equation

$$\frac{d}{dt}N(t) = -\alpha N(t) - \beta \int n^2(r, t) d^3r + \mathcal{O}(n^3). \quad (1)$$

The experimental fluorescence data is fitted to a solution of this equation. No absolute calibration of the atom number is required for the determination of the decay constant  $\alpha$ . In Fig. 1, non-exponential two-body decay due to intra-trap collisions can be seen during the first 30 seconds. Two-body losses depend on the integral over the local number density  $n(r, t)$  and are described by the parameter  $\beta$ , the absolute determination of which would require an absolute calibration of  $n(r, t)$ , which is not the scope of this work. An uncalibrated value of  $\beta$ , however, is determined in our fitting procedure. For all data runs no contributions of order  $n^3$  or higher could be observed.

At low atom numbers the decay is dominated by one-body losses with rate

$$\alpha = \frac{1}{\tau_2} (1 - \pi_3) + \frac{1}{\tau_3} \pi_3 + \gamma p + \mathcal{ML}. \quad (2)$$

The parameter  $\pi_3$  gives the population in the  $^3\text{D}_3$ -state. Thus  $(1 - \pi_3)N$  atoms decay from the  $^3\text{P}_2$ -state with lifetime  $\tau_2$ . The combined rate for all decay channels from the  $^3\text{D}_3$ -state other than the transition to the  $^3\text{P}_2$ -state (see Fig. 2) is given by  $\tau_3^{-1}$ . Background collisions contribute with a rate of  $\gamma p$  [16] with  $p$  being the pressure in the vacuum chamber and  $\gamma$  being a constant depending on the atomic and molecular species present. The parameter  $\mathcal{ML}$  summarizes possible MOT losses. The main objective of this work is to determine the lifetime  $\tau_2$  from the observed decay rates  $\alpha$  by extrapolating to vanishing excitation ( $\pi_3 = 0$ ), background pressure ( $p = 0$ ), and MOT losses ( $\mathcal{ML} = 0$ ). Achieving optimized starting conditions (small  $\pi_3$  and  $p$ ) and minimizing potential contributions of  $\mathcal{ML}$  by a systematic analysis of the MOT characteristics have been essential.

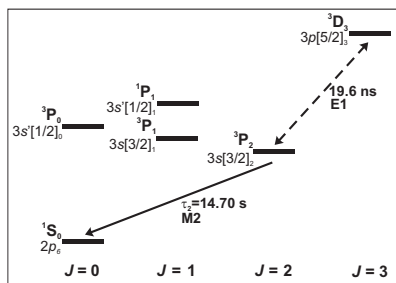


FIG. 2: Detail of the level scheme of neon. Atomic levels are labeled according to LS- and Racah notation. Transitions are labeled by their multipolar character.

Following [17], the population  $\pi_3$  is determined by:

$$\pi_3 = \frac{1}{2} \frac{C \cdot I/I_0}{1 + C \cdot I/I_0 + (2\Delta/\Gamma)^2}. \quad (3)$$

with the total intensity  $I$  of the MOT light fields, the saturation intensity  $I_0 = \pi\hbar c\Gamma/3\lambda^3 = 4.08 \text{ mW/cm}^2$  (linewidth  $\Gamma = 2\pi \times 8.18 \text{ MHz}$ ,  $\lambda = 640.4 \text{ nm}$ ) and detuning  $\Delta$ . The phenomenological parameter  $C$  accounts for the deviation of the effective total intensity in a three-dimensional MOT from a one-dimensional two-level system [17]. We adopt the notion of [3] and take  $C = 0.7$  with an uncertainty of 0.3. The intensity  $I$  is measured with an uncertainty of 10 %, the detuning  $\Delta$  with an absolute uncertainty of 1 MHz. Therefore, for all data presented here the uncertainty in  $C$  is the dominant contribution to the uncertainty in  $\pi_3$ .

The experimental setup is shown in Fig. 3. A collimated beam of metastable atoms is decelerated in a Zeeman-slower with the slowing laser beam passing through the center of the MOT. The MOT light field consists of six individual beams (diameter 22 mm) with spatially filtered beam profiles. All light fields are derived from a dye laser which is frequency stabilized to a neon RF-discharge.

For each run, the MOT is loaded for 400 ms reaching a number of up to  $4 \times 10^8$  atoms, a maximum collision-limited density on the order of  $1 \times 10^9 \text{ cm}^{-3}$  and a typical temperature below 1 mK. Then, the loading process is terminated by blocking the atomic beam and the slowing laser beam by mechanical shutters, and by switching off the magnetic field of the Zeeman slower. In the following measurement period of two minutes, the fluorescence of the trapped atoms is recorded by a CCD camera capturing five image frames per second. Fluorescence decay curves are obtained by integrating the counts of each frame over the region where atoms are present. Great care has been taken to eliminate the influence of residual stray light. The decay curves span up to four orders of magnitude in signal. Fig. 1 shows two sets of data taken for different values of  $\pi_3$ . For  $\pi_3 = 0.005$  a decay rate of  $\alpha = 0.06929(48) \text{ s}^{-1}$  and a respective decay time of  $\alpha^{-1} = 14.43 \text{ s}$  is observed.

In the following sections we describe our procedure to extrapolate the observed decay rate  $\alpha$  to the  $^3\text{P}_2$  decay rate  $\tau_2^{-1}$ . For the extrapolation of  $\alpha$  to vanishing background pressure a systematic investigation of the

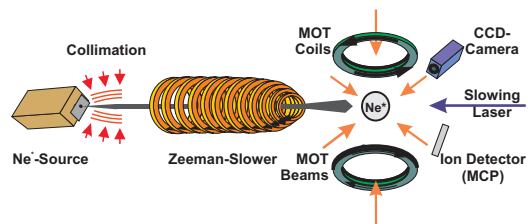


FIG. 3: Experimental setup.

MOT decay as a function of pressure has been carried out (Fig. 4(a)). The pressure is given as the nominal reading of the vacuum gauge (Balzers IKR070). The specific composition of the background gas is not known. However, we could observe a linear dependence of  $\alpha$  on pressure over a range of almost two orders of magnitude, indicating a pressure-independent composition of the background gas. From a linear fit for data taken for  $\pi_3 < 0.1$ , we can determine the slope  $\gamma = 5.2(1) \times 10^7 \text{ mbar}^{-1} \text{ s}^{-1}$ . As a special feature of our setup, we can directly determine a possible offset by simultaneously measuring the fluorescence and the rate of ions produced by collisions using a multichannel plate (MCP) ion detector. Under typical operating conditions we detect ions of different origin: (a)  $\text{Ne}^+$ -ions originating from intra-trap collisions (rate  $\propto \int n^2(r, t) d^3r$ ). (b) Ions which originate from collisions of metastable neon atoms with residual gas constituents (rate  $\propto N(t) \times p$ ). Thus, the ion count rate  $R_{\text{ion}}(t)$  can be modelled by

$$R_{\text{ion}}(t) = c_1 N(t) + c_2 \int n^2(r, t) d^3r, \quad (4)$$

where  $c_1$  is assumed to be proportional to  $p$ . The values of  $c_1$  obtained for different pressures are shown in Fig. 4(b). From a linear fit we can determine the offset of the pressure gauge reading to  $(4 \pm 7) \times 10^{-12} \text{ mbar}$  also allowing for a vanishing offset. By combining the results for  $\gamma$  and the offset, we can extrapolate the observed decay rates to  $p = 0$ . Due to the already low background pressure for our decay measurements only small corrections arise: At  $p = 5 \times 10^{-11} \text{ mbar}$  the background collision rate of  $\gamma p = 1/(420 \text{ s})$  is more than a factor of 25 smaller than the observed decay rate  $\alpha$ .

We also investigated the possibility of additional atom losses from the MOT (contribution  $\mathcal{ML}$  in Eq. (2)) attributed to a finite trap depth  $U_0$  or finite escape velocity  $v_e$  [18]. We assume that a lossless MOT would result from an infinite trapping volume leading to infinite  $U_0$  and  $v_e$ . In principle, this could be achieved for the applied magnetic field gradient  $B'$  approaching zero if the MOT beams could be made infinitely large. In all practi-

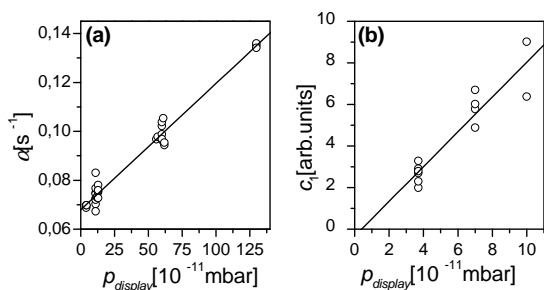


FIG. 4: (a) Decay rates  $\alpha$  obtained for  $\pi_3 < 0.1$  after extrapolation to  $\pi_3 = 0$  as a function of the nominal background pressure  $p_{\text{display}}$ . (b) Coefficients  $c_1$  proportional to the number of ionizing background collisions as a function of  $p_{\text{display}}$  allowing the determination of the vacuum gauge offset.

cal implementations the trap depth will remain finite due to the finite size of the laser beams. Thus, for a given beam geometry, a variation in  $B'$  should allow to investigate the MOT stability and to quantify the MOT losses  $\mathcal{ML}$  which include diffusive motion out of the trapping volume [19] leading to an exponentially decreasing loss rate with increasing trap depth and non-ionizing background gas collisions [16] already being accounted for by the  $p \rightarrow 0$  extrapolation. The influence of the magnetic field gradient on the measured decay rate  $\alpha$  is shown in Fig. 5 for two values of  $\pi_3 = 0.016$  and  $0.41$ , respectively.

In the most relevant case of small  $\pi_3$  (Fig. 5(a)), for sufficiently large  $B' > 10 \text{ G/cm}$  a variation of  $B'$  does affect the measured  $\alpha$  not more than the uncertainties obtained from the fit. Thus we conclude that for our operating regime (shaded region in Fig. 5(a)) the trap depth  $U_0$  and escape velocity  $v_e$  are sufficiently large and that potential MOT loss contributions to the decay rate  $\alpha$  are not significant. For large  $\pi_3$  (Fig. 5(b)), a variation of the MOT stability with  $B'$  is observed. Unfortunately, no quantitative model of the MOT at high saturation exists, the application of the loss models discussed above is not straightforward, and only a minimum and a maximum estimate of  $\mathcal{ML}$  can be given: Since our decay data for large  $\pi_3$  have been taken at  $B' = 1.5 \text{ G/cm}$  which gives the best MOT stability, it is not clear whether MOT losses have a significant contribution on the determination of  $\alpha$  at all. On the other hand, a linear extrapolation of  $\alpha$  to  $B' = 0$  should overestimate the corrections to be made [16, 19] giving  $\mathcal{ML} = 0.005(2) \text{ s}^{-1}$  as an upper limit. Losses for large  $\pi_3$  only influence the  $\pi_3 \rightarrow 0$  extrapolation which we take into account by incorporating  $0 \text{ s}^{-1} < \mathcal{ML} < 0.005 \text{ s}^{-1}$  into the uncertainties of this extrapolation.

After this systematic study of the influence of background collisions and MOT losses the determination of the  $^3\text{P}_2$  lifetime  $\tau_2$  can be obtained by extrapolating the measured decay rates to vanishing population  $\pi_3$ . Only data for a pressure below  $5 \times 10^{-11} \text{ mbar}$  are considered and an extrapolation to  $p = 0$  is performed. The dependence of  $\alpha_{p=0}$  on  $\pi_3$  is shown in Fig. 6 exhibiting a sim-

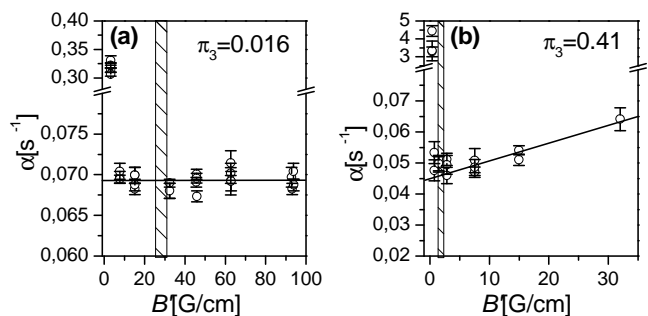


FIG. 5: Systematic investigation of MOT losses. Decay rates are plotted as a function of the magnetic field gradient for two different excitations (a)  $\pi_3 = 0.016$  and (b)  $\pi_3 = 0.42$ . Shaded areas indicate the gradients of typical operating conditions.

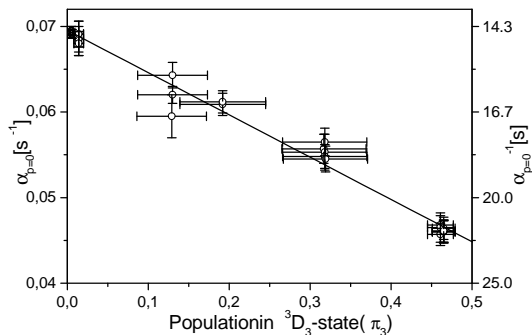


FIG. 6: Decay rates  $\alpha_{p=0}$  as a function of the excitation  $\pi_3$  allowing the determination of  $\tau_2$  in the limit of  $\pi_3 \rightarrow 0$ .

TABLE I: Contributions to the  $\tau_2 = 14.70(13)$ s extrapolation.

MOT decay at $\pi_3 = 0.005$	$0.06929 \text{ s}^{-1}$	$\pm 0.00048 \text{ s}^{-1}$
$\pi_3 \rightarrow 0$ -extrapolation	$+0.00028 \text{ s}^{-1}$	$\pm 0.00013 \text{ s}^{-1}$
$p \rightarrow 0$ -extrapolation	$-0.00156 \text{ s}^{-1}$	$\pm 0.00037 \text{ s}^{-1}$
$1/\tau_2$	$0.06801 \text{ s}^{-1}$	$\pm 0.00062 \text{ s}^{-1}$

ple linear behavior. Displayed uncertainties in  $\alpha_{p=0}$  are given by the combined uncertainties in the fit of  $\alpha$  and uncertainties in the  $p \rightarrow 0$  extrapolation. To minimize uncertainties in the  $\pi_3 \rightarrow 0$  extrapolation, only data sets for  $\pi_3 < 0.05$  and  $\pi_3 > 0.4$  showing the smallest absolute uncertainties in  $\pi_3$  have been included. The final value of the  $^3\text{P}_2$  lifetime and decay rate are  $\tau_2 = 14.70(13)$  s and  $\tau_2^{-1} = 0.06801(62)$  s, respectively. Table I gives a summary of contributions and uncertainties for these values. Since stable MOT conditions are directly accessible for  $\pi_3 = 0.005$  and  $p < 5 \times 10^{-11}$  mbar only unprecedented small corrections are required. The final value for  $\tau_2$  only deviates from the uncorrected value of  $\alpha^{-1} = 14.43$  s by

2 %.

In addition to this result, extrapolating  $\alpha_{p=0}$  to  $\pi_3 = 1$ , that is to a hypothetical total population transfer to the  $^3\text{D}_3$ -state, is also possible. From this, we gain the first experimentally determined lower limit of  $\tau_3 \geq 59$  s for the combined rate  $\tau_3^{-1}$  of decay of the  $^3\text{D}_3$ -state via all channels except the direct decay to the  $^3\text{P}_2$  state. However, this value depends sensitively on the  $\mathcal{ML}$ -correction applied for large  $\pi_3$  and only the stated lower limit is accessible.

To conclude we would like to compare our result of  $\tau_2 = 14.70(13)$  s to theoretical values obtained by different atomic structure calculations. Prior to our work, published theoretical values were given in [20] to 24.4 s, which can be rescaled to 20.0 s using more accurate input parameters, and in [21] to 22 s. Significant remaining discrepancies initiated a reexamination of atomic structure calculations for the whole set of  $^3\text{P}_2$  lifetimes of rare-gas atoms. A preliminary result based on a multiconfiguration Dirac-Fock calculation gives a value of 18.9 s for neon [10]. A high degree of sensitivity to the included electron correlations has been found. Theoretical values are still expected to be larger than the experimental value, since the inclusion of additional electron correlations should further reduce the calculated lifetime. Refined calculations are forthcoming [10]. Most recent ab-initio calculations using MCHF methods give a lifetime of 16.9 s [22]. Considering the combined progress in experiment and theory, we anticipate that the determination of the  $^3\text{P}_2$  lifetime of neon may continue to serve as an important test for precision atomic structure calculations in the future.

We thank Y.-K. Kim for valuable discussions and are grateful for financial support by the DFG within the *Schwerpunktprogramm SPP 1116*.

- 
- [1] The notation of states throughout this paper is based on LS-coupling. Racah notation is included in Fig. 2.
- [2] see e.g. <http://weak0.physics.berkeley.edu/weakint/research/neon/>.
- [3] S.J.M. Kuppens et al., Phys. Rev. A **65**, 023410 (2002).
- [4] M. Zinner, Ph.D. thesis, unpublished (2002); [http://www.iqo.uni-hannover.de/html/ertmer/atom\\_optics/nebec/nebec.html](http://www.iqo.uni-hannover.de/html/ertmer/atom_optics/nebec/nebec.html).
- [5] F.M. Penning, Naturwissenschaften **15**, 818 (1927);
- [6] A. Robert et al., Science **292**, 461 (2001).
- [7] F. Pereira Dos Santos et al., Phys. Rev. Lett. **86**, 3459 (2001).
- [8] M. Yasuda, F. Shimizu, Phys. Rev. Lett. **77**, 3090 (1996); E.A. Burt et al., Phys. Rev. Lett. **79**, 337 (1997); W. Ketterle, H.J. Miesner, Phys. Rev. A **56**, 3291 (1997).
- [9] J.J. Hope, C.M. Savage, Phys. Rev. A **54**, 3177 (1996).
- [10] J.P. Desclaux, P. Indelicato, and Y.-K. Kim, private communication (2002).
- [11] F. Shimizu, Laser Spectroscopy IX, Academic Press, p. 444 ff, (1989).
- [12] F. Shimizu, private communication.
- [13] H. Katori, F. Shimizu, Phys. Rev. Lett. **70**, 3545 (1993).
- [14] J. Lefers et al., Phys. Rev. A **66**, 012507 (2002).
- [15] M. Walhout, A. Witte, and S.L. Rolston, Phys. Rev. Lett. **72**, 2843 (1994).
- [16] A.M. Steane, M. Chowdhury, and C.J. Foot, J. Opt. Soc. Am. B **6**, 2142 (1992).
- [17] C.G. Townsend et al., Phys. Rev. A **52**, 1423 (1995).
- [18] J. Weiner et al., Rev. Mod. Phys. **71**, 1 (1999).
- [19] P.A. Willems et al., Phys. Rev. Lett. **78**, 1660 (1997).
- [20] N.E. Small-Warren, L.-Y. Chow-Chiu, Phys. Rev. A **11**, 1777 (1975).
- [21] J.P. Desclaux, P. Indelicato, Y.-K. Kim, cited in [15].
- [22] G. Tachiev, C. Froese Fischer (2002), <http://atoms.vuse.vanderbilt.edu>.